

A. Yu. Konobeyev, U. Fischer and P. E. Pereslavytsev

Evaluation of advanced displacement cross-sections for the major EUROFER constituents based on an atomistic modelling approach

The displacement cross-sections were evaluated for main components of EUROFER at the energies of primary neutrons up to 150 MeV. The number of primary defects was calculated using an advanced binary collision approximation model applying results of molecular dynamics simulations. The cross-sections obtained were processed into ENDF and ACE formatted data and tested using the MCNP code.

Auswertung fortgeschrittener Verlagerungsquerschnitte für Grundkomponenten von EUROFER auf der Basis eines atomistischen Modellansatzes. Verlagerungsquerschnitte für Grundkomponenten von EUROFER wurden für Neutronenenergien bis 150 MeV ausgewertet. Die Anzahl der stabilen Defekte wurde mit Hilfe eines weiterentwickelten binären Stoßapproximation-Modells mit einer nachfolgenden Korrektur auf der Basis der Simulationen der molekularen Dynamik berechnet. Die berechneten Wirkungsquerschnitte wurden in ENDF- und ACE-Daten umgewandelt und mit Hilfe von MCNP getestet.

1 Introduction

Reliable assessments of radiation induced damage in fusion reactor materials require the use of advanced simulation techniques for the underlying displacement damage mechanisms. The calculation of radiation damage rates for the EUROFER reduced activation steel will be, therefore, based on improved displacement cross-sections based on molecular dynamics (MD) and binary collision approximation (BCA) simulation methods for the calculation of the number of lattice defects. This approach shows a better agreement [1, 2] with experimental data of point-defect production in materials that the standard Norgett-Robinson-Torrens (NRT) approximation [3] implemented in commonly used codes like the NJOY code [4].

In the present work neutron induced damage energy and displacement cross-section data were evaluated for the main EUROFER constituents up to 150 MeV utilizing the advanced atomistic modelling approach. The data obtained were processed into ENDF and ACE formatted data and tested by means of MCNP calculations.

The displacement cross-section is calculated according to the following general expression

$$\sigma_d(E_n) = \sum_i \int_{E_d}^{T_i^{\max}} \frac{d\sigma(E_n, Z_T, A_T, Z_i, A_i, T_i)}{dT_i} \eta(Z_T, A_T, Z_i, A_i, T_i) N_{\text{NRT}}(Z_T, A_T, Z_i, A_i, T_i) dT_i, \quad (1)$$

where E_n is the incident neutron energy; $d\sigma/dT_i$ is the energy distribution of i -th primary knock-on atom (PKA) with the kinetic energy T formed in the nuclear reaction; Z and A are the atomic and the mass numbers, “T” and “i” relates to the target and the recoil atom, correspondingly, for the elastic scattering $Z_i = Z_T$, $A_i = A_T$; N_{NRT} is the number of Frenkel pairs predicted by the NRT model, η is the defect production efficiency [5]; E_d is the effective threshold displacement energy; T_i^{\max} is the maximal kinetic energy of the PKA produced in i -th reactions; the summation is over all recoil atoms produced in the irradiation.

The η -value in Eq. (1) reflects the deviation of the number of stable defects obtained in simulations or experiments from the number N_{NRT} predicted by the NRT model. The value N_{NRT} is calculated as follows

$$N_{\text{NRT}} = 0.8 \cdot T_{\text{dam}} / (2E_d), \quad (2)$$

where T_{dam} is the “damage energy” equal to the energy transferred to lattice atoms reduced by the losses for electronic stopping of atoms in the displacement cascade [6]:

$$T_{\text{dam}}(T) = \frac{T}{1 + k g(\varepsilon)} \quad (3)$$

$$g(\varepsilon) = 3.4008\varepsilon^{1/2} + 0.40244\varepsilon^{3/4} + \varepsilon, \quad (4)$$

$$k = \frac{32}{3\pi} \left(\frac{m_e}{M_T} \right)^{1/2} \frac{(A_i + A_T)^{3/2} Z_i^{2/3} Z_T^{1/2}}{A_i^{3/2} (Z_i^{2/3} + Z_T^{2/3})^{3/4}}, \quad (5)$$

$$\varepsilon = [A_T T / (A_i + A_T)] [a / (Z_i Z_T e^2)], \quad (6)$$

$$a = a_0 (9\pi^2 / 128)^{1/3} (Z_i^{2/3} + Z_T^{2/3})^{-1/2}, \quad (7)$$

where m_e is the mass of an electron, a_0 is the Bohr radius, M_T is the mass of the atom of target material and the other values are defined above, “e” is the electron charge; the kinetic energy T of PKA is taken in keV; the value of “k” is defined according to Ref. [6] and for the case of $Z_i = Z_T$, $A_i = A_T$ it coincides with the NRT-value equal to $k = 0.1337 Z_i^{1/6} (Z_i / A_i)^{1/2}$.

The method of the calculation of the number of stable displacements and recoil energy distributions is described below in the Section 2.

2 Brief description of the method of calculation of displacement cross-section

2.1 Recoil energy distributions

The preliminary calculations were performed to check the consistency of the data planned to be used as the origin of

recoil energy distribution and to study the influence of the $d\sigma/dT$ data on the calculated displacement cross-sections.

The recoil energy distributions were calculated using the NJOY code [4] and processed using the SPKA code [7].

The typical difference of recoil energy distributions obtained using data from different nuclear data libraries is shown in Figs. 1–4. Fig. 1 illustrates $d\sigma/dT$ values at the primary neutron energy 1 MeV, Fig. 2 at 5 MeV, Fig. 3 at 14.5 MeV, and Fig. 4 at 150 MeV. Figs. 1–3 show the recoil energy distribution for the elastic scattering, the total distribution, and $d\sigma/dT$ for a number of reactions. Fig. 4 shows the recoil energy distributions for all nonelastic interactions for ^{56}Fe . For the comparison Figs. 3, 4 illustrates also the nonelastic contribution to the recoil energy distributions calculated using intranuclear cascade evaporation models implemented in DISCA-C [8] and CASCADE [9] codes. The use of DISCA-C at relative low energy 14.5 MeV was justified due to modifications discussed in Ref. [8].

Figs. 1–4 show a relative large difference between recoil energy distributions obtained using data from different nuclear libraries and calculations.

The choice of the origin of reliable data for $d\sigma/dT$ should take into account that the measured data for recoil spectra are not available and, as additional calculations show, the specific shape of the recoil energy distribution has a relatively small impact on calculated displacement cross-sections. For this reason, a preference has to be given to libraries containing neutron data, evaluated using the latest sets of measured data and results of advanced calculations. In the present work, the recoil energy distributions were prepared using JEFF-3.2T2, TENDL-2011, and TENDL-2012 data.

2.2 Number of stable displacements

The method of the calculation of the number of displacements is briefly described below. The details can be found in Refs. [1, 2]. The binary collision approximation model is applied for the simulation of atomic collision for an ion moving in the material up to its certain minimal kinetic energy T_{crit} . Below this energy the BCA simulation is interrupted and the number of defects is estimated using results of molecular dynamics calculations.

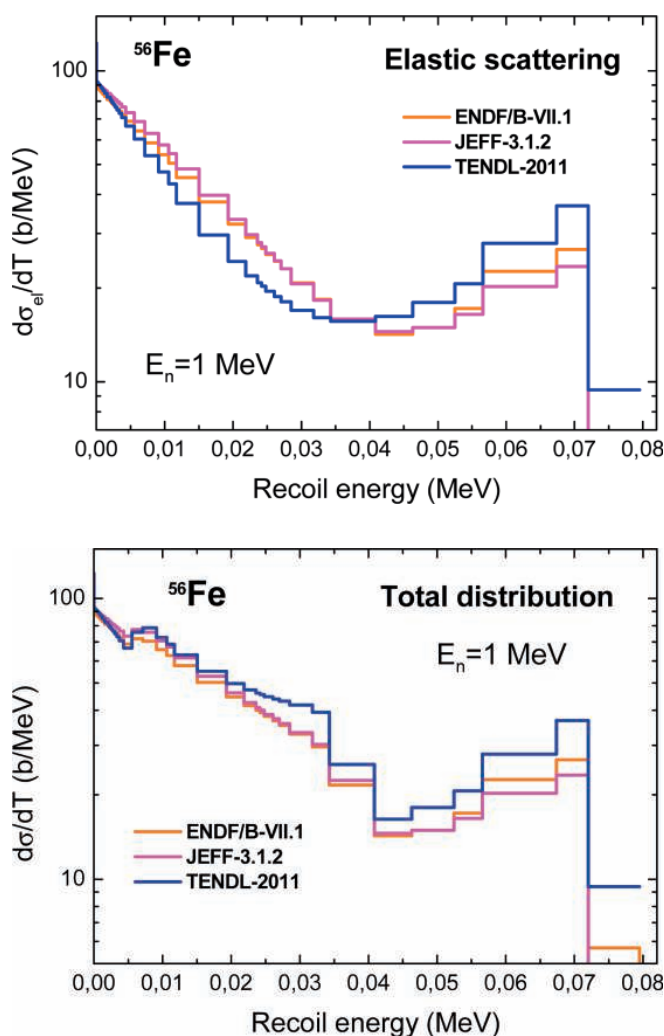


Fig. 1. Examples illustrating difference of recoil energy distributions for ^{56}Fe obtained using data from various neutron data libraries. Recoil energy distributions were calculated for the primary neutron energy equal to 1 MeV

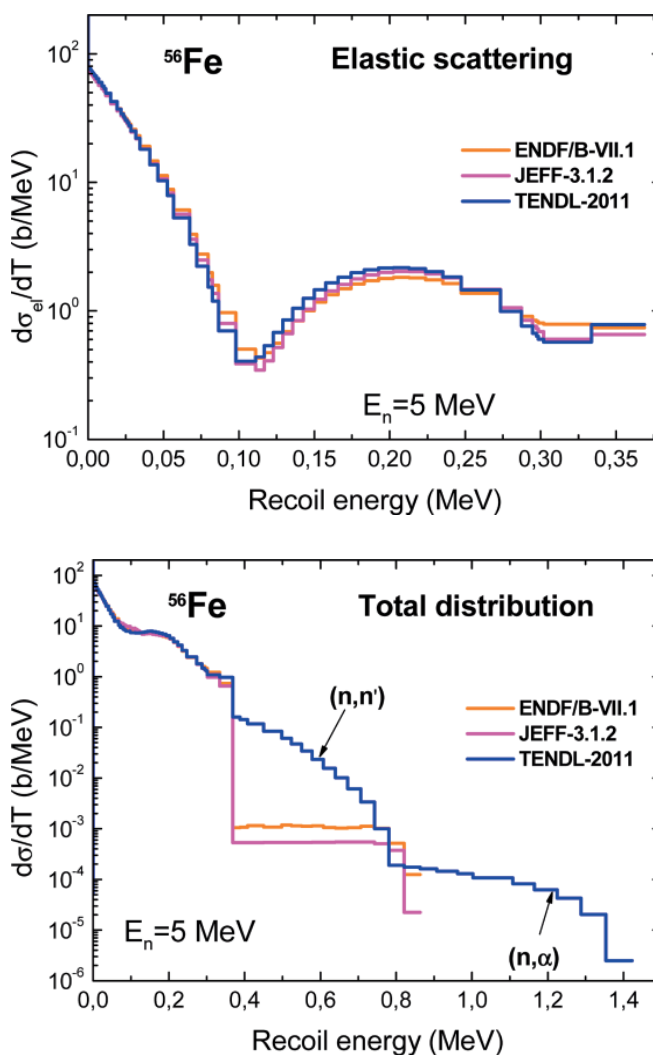


Fig. 2. Examples illustrating difference of recoil energy distributions for ^{56}Fe obtained using data from various neutron data libraries. Recoil energy distributions were calculated for the primary neutron energy equal to 5 MeV

The differential cross-section for the transfer of the kinetic energy T from the primary ion to the lattice atom $d\sigma^{Tr}(E, T)$ in BCA simulation was calculated as follows

$$d\sigma_i^{Tr}(E, T) = \pi a^2 f(t^{1/2}) \frac{dt}{2t^{3/2}}, \quad (8)$$

where “ a ” is defined by Eq. (7) and the function $f(t^{1/2})$ is equal to

$$f(t^{1/2}) = \lambda t^{1/2-m} \left[1 + (2\lambda t^{1-m})^q \right]^{-1/q}, \quad (9)$$

the λ , m , q are taken from Ref. [10].

In the present work the number of defects produced by ions with the kinetic energy below T_{crit} was estimated according to MD simulations for iron-chromium alloys made by Vörtler et al. [11]. It is supposed that the possible consideration of other impurities of EUROFER has no impact on the final results. The assumption is confirmed by the global comparison of MD simulations and experimental data for different materials [5]. The energy T_{crit} was taken about 61 keV, which corresponds to the “critical” damage energy equal to 40 keV for EUROFER. The last value is considered as the highest energy where the results of MD simulations [11] can be applied. The BCA calculations were performed using the IOTA code elaborated in KIT [12].

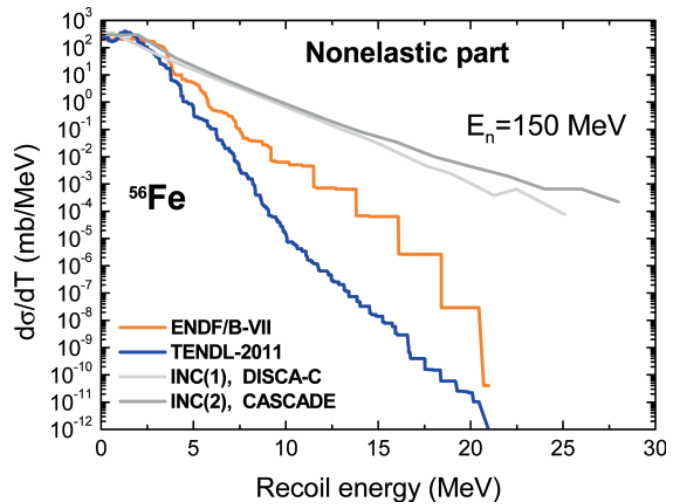


Fig. 4. Examples illustrating difference of recoil energy distributions for nonelastic neutron interactions with ^{56}Fe obtained using data from various neutron data libraries and calculated using intranuclear cascade evaporation model, see explanations in the text

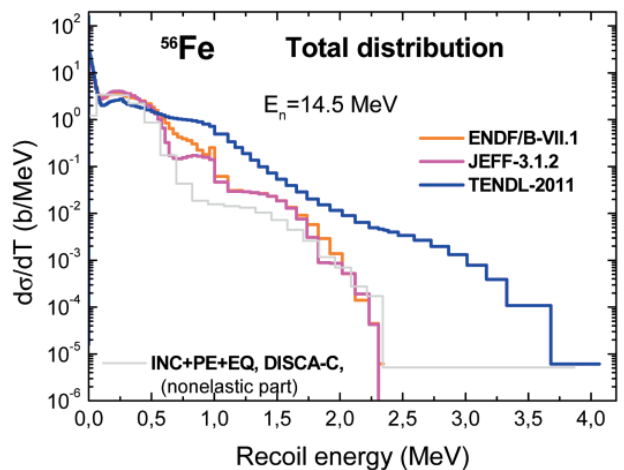
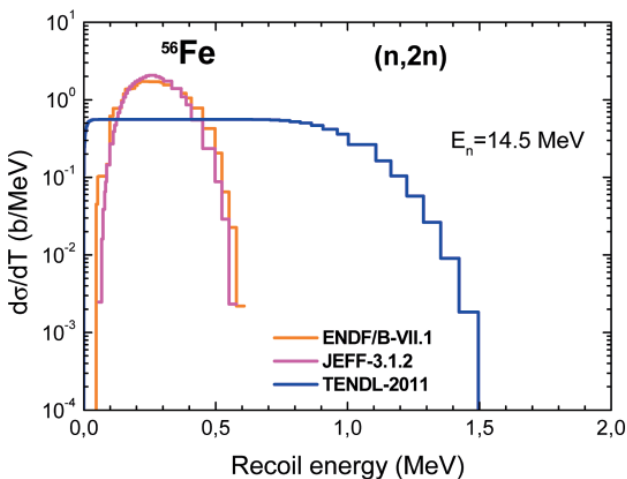
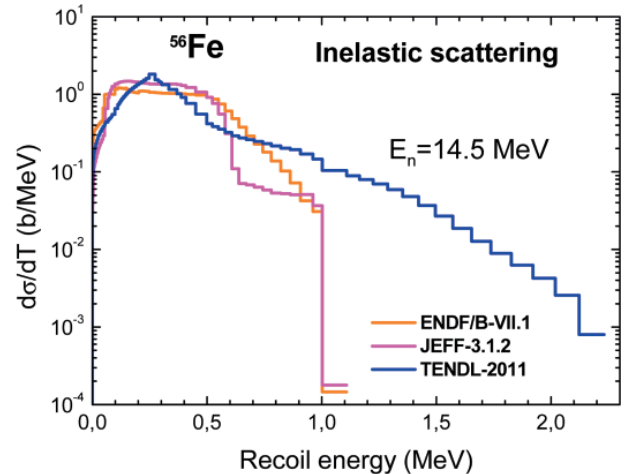
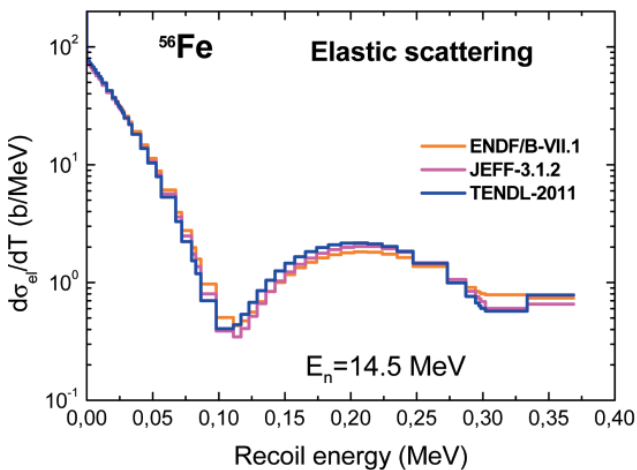


Fig. 3. Examples illustrating difference of recoil energy distributions for reactions induced by 14.5 MeV – neutrons at ^{56}Fe irradiation obtained using data from various neutron data libraries and calculated using the DISCA-C code, see explanations in the text

The example of the efficiency of the defect generation $\eta(T)$ for Fe-ions is shown in Fig. 5 depending on the damage energy T_{dam} . The maximal value of T_{dam} presented on Fig. 5 corresponds to the kinetic energy of primary ions equal to 1 GeV.

Fig. 6 shows the number of stable defects N_F produced by Fe-ion irradiation in iron-chromium alloys calculated using BCA-MD approach together with results of Ref. [11]. The variation of the chromium content up to 15 % seems have no influence on calculated values. For the comparison results of two independent BCA simulations without MD-corrections were added to Fig. 6. For these calculations the special value of E_d energy was selected for TRIM [13] and IOTA codes reproducing the N_F value from MD modeling at the highest energy of simulation [11]. Such reproduction is possible at rather unphysical E_d values exceeding 300 eV, which demonstrates the limited possibilities of pure BCA simulations as a reliable model for displacement cross-section calculations in a wide energy range of primary particles.

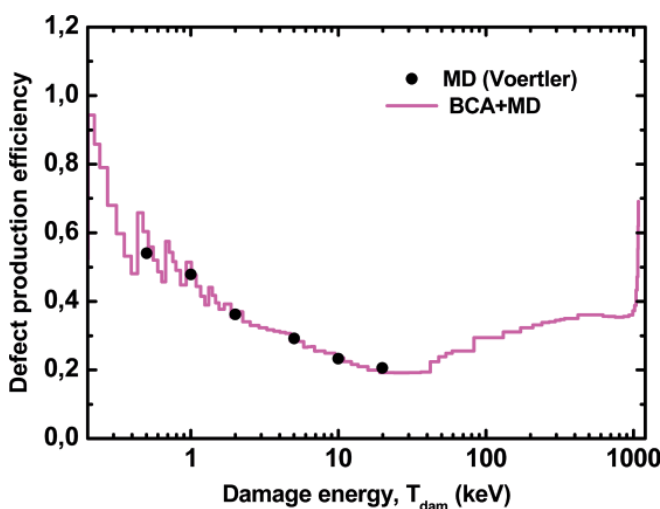


Fig. 5. The efficiency of the defect production for the Fe-iron of iron-chromium alloys obtained using the combined BCA, MD method and results of the MD simulation [11]

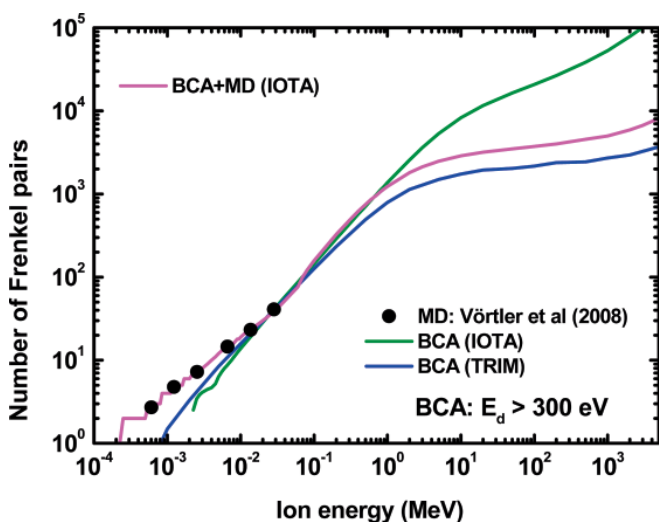


Fig. 6. The number of stable defects calculated for the Fe-iron of iron-chromium alloys using the combined BCA-MD method, two BCA models, and results of the MD simulation [11], see explanations in the text

The values of $\eta(T)$ obtained using BCA-MD approach were introduced in the NJOY code [4], which required the modification of the DF-function in the code.

3 Evaluation of displacement cross-section for EUROFER

The calculations of σ_d values were performed using the recoil energy distributions obtained applying data from neutron data libraries discussed in Section 2.1 and results of BCA-MD simulations performed with the help of the IOTA code, as discussed in Section 2.2. For the comparison, also, calculations of displacement cross-sections were carried out using the NRT model, i. e. with $\eta(T) = 1$, Eq. (1). In all calculations, the E_d value was taken equal to 40 eV.

The evaluation procedure consisted of the removing of possible peculiarities in σ_d values resulting from the use of $d\sigma/dT$ taken from neutron data libraries, especially at 20 MeV, the fitting to results of σ_d calculations using intranuclear cascade evaporation models above 150 MeV [1, 2], and the combination of the different results below and above 20 MeV, if necessary.

Figs. 7–9 show examples of calculated and evaluated displacement cross-sections for a number of EUROFER constituents. The preference of the origin of $d\sigma/dT$ data below the neutron energy 20 MeV was given to JEFF-3.2T2 and above 20 MeV to TENDL-2011 and TENDL-2012. An advantage of TENDL is the agreement of the corresponding σ_d values and results of calculation applying the intranuclear cascade evaporation models [1, 2] at primary particle energies above 150 MeV.

The final σ_d values for EUROFER consists of the summing of the displacement cross-sections for ten components, giving main contributions to the steel composition, Fe, Cr, W, Mn, V, Ta, C, Si, N, and Zr. Obtained values are shown in Fig. 10 both for BCA-MD and NRT model. The calculations with the NRT model was performed using the common procedure implying the weighted summing of σ_d for independent materials and using the original version of NJOY.

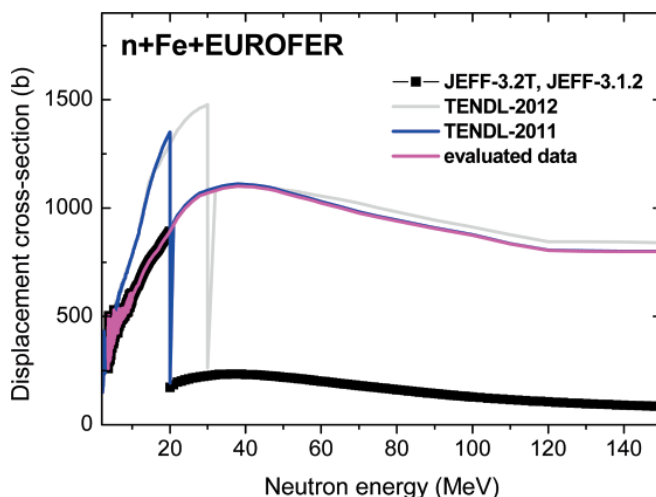


Fig. 7. Example of displacement cross-section calculated for iron in EUROFER calculated using data from various nuclear libraries. The calculations were performed with $\eta(T) = 1$, Eq. (1)

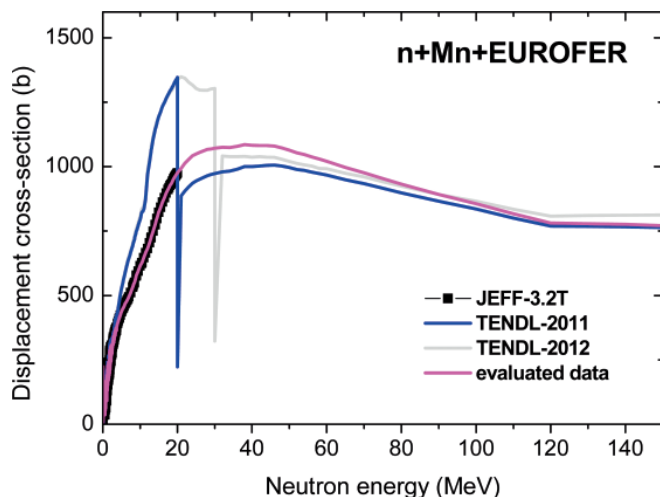


Fig. 8. Example of displacement cross-section calculated for manganese in EUROFER calculated using data from various nuclear libraries. The calculations were performed with $\eta(T) = 1$

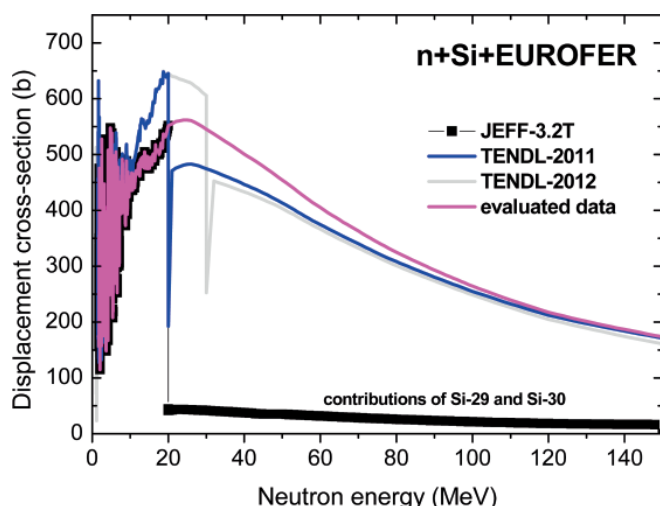


Fig. 9. Example of displacement cross-section calculated for silicon in EUROFER calculated using data from various nuclear libraries. The calculations were performed with $\eta(T) = 1$

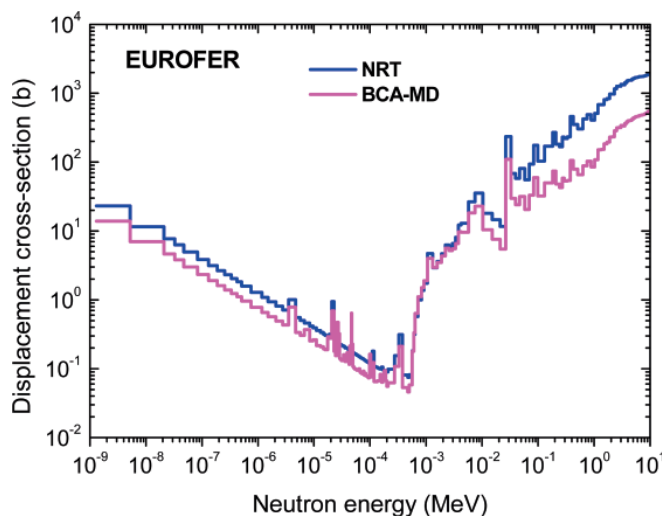


Fig. 10. Displacement cross-sections for EUROFER evaluated using the BCA-MD approach and the NRT model. For the clarity the data on the figure are averaged using a number of energy groups

4 Data in ENDF and ACE format

The data obtained were written in ENDF format. Because of results of the BCA-MD modelling are absolute numbers of stable displacements, the final values were recorded as cross-sections in barn units. This data representation is different from the common recording of “damage energy production cross-sections” with MT = 444 by the NJOY processing. In the latter case, the displacement cross-section varies according to the E_d value, which is not reasonable for current results. The resulting cross-section were recorded in the file MF = 3, the section MT = 900, which number was adopted in the present work to record such kind of data.

The file obtained was processed with NJOY recording the data in the ACE format. The resulting file was tested with the help of the MCNP code [14] calculations to avoid possible inconsistencies in the data representation.

5 Conclusion

The displacement cross-sections were evaluated for main EUROFER constituents at the primary neutron energies up to 150 MeV. The recoil energy distributions were calculated using data from JEFF-3.2T2, TENDL-2011, and TENDL-2012. The number of primary defects was calculated using an advanced binary collision approximation model applying results of molecular dynamics simulations. The cross-sections obtained were written in ENDF format, processed into ACE formatted data, and tested using the MCNP code.

The data obtained can be applied for the evaluation of realistic radiation damage rate in EUROFER irradiated with neutrons in various units including the fission reactor.

Acknowledgements

This work has been supported by Fusion for Energy (F4E), Barcelona, under the specific grant agreement F4E-FPA-168.01. The views and opinions expressed herein reflect only the author's views.

(Received on 5 December 2014)

References

- 1 Konobeyev, A. Yu.; Broeders; C. H. M.; Fischer, U.: Improved displacement cross sections for structural materials irradiated with intermediate and high energy protons. Proc. 8th International Topical Meeting on the Nuclear Applications of Accelerator Technology (AccApp'07), July 30–August 2, 2007, Pocatello, Idaho, USA, p.241
- 2 Konobeyev, A. Yu.; Fischer, U.; Zanini, L.: Advanced evaluations of displacement and gas production cross sections for chromium, iron, and nickel up to 3 GeV incident particle energy. Tenth International Topical Meeting on Nuclear Applications of Accelerators (AccApp'11), Knoxville, TN April 3–7, 2011
- 3 Norgett, M. J.; Robinson; M. T.; Torrens, I. M.: A proposed method of calculating displacement dose rates. Nucl. Eng. Des. 33 (1975) 50, DOI:10.1016/0029-5493(75)90035-7
- 4 NJOY: Data processing system of evaluated nuclear data files in ENDF format, <https://www.oecd-neo.org/dbprog/njoy-links.html>
- 5 Broeders, C. H. M.; Konobeyev, A. Yu.: Defect production efficiency in metals under neutron irradiation. J. Nucl. Mater. 328 (2004) 197, DOI:10.1016/j.jnucmat.2004.05.002
- 6 Robinson, M. T.: Basic physics of radiation damage production. J. Nucl. Mater. 216 (1994) 1; and references on older works of M. T. Robinson therein, DOI:10.1016/0022-3115(94)90003-5
- 7 Simakov, S.: KIT, private communication
- 8 Broeders, C. H. M.; Konobeyev, A. Yu.; Korovin, Yu. A.; Sosnin V. N.: DISCA – advanced intranuclear cascade cluster evaporation model

- code system for calculation of particle distributions and cross sections, FZKA 7221 (2006); <http://d-nb.info/98154746X/34>
- 9 Barashenkov, V. S.: Monte Carlo simulation of ionization and nuclear processes initiated by hadron and ion beams in media, *Comp. Phys. Comm.* 126 (2000) 28, DOI:10.1016/S0010-4655(99)00417-8
 - 10 Winterbon, K. B.; Sigmund, P.; Sanders, J. B. K.: Spatial distribution of energy deposited by atomic particles in elastic collisions. *K. Dan. Vidensk. Selsk. Mat. Fys. Medd.* 37, N14 (1970)
 - 11 Vörtler, K.; Björkas, C.; Terentyev, D.; Malerba, L.; Nordlund, K.: The effect of Cr concentration on radiation damage in Fe–Cr alloys. *J. Nucl. Mat.* 382 (2008) 24, DOI:10.1016/j.jnucmat.2008.09.007
 - 12 Broeders, C. H. M.; Konobeyev, A. Yu.; Voukelatou, K.: IOTA – a code to study ion transport and radiation damage in composite materials, FZKA 6984 (2004), <http://bibliothek.fzk.de/zb/berichte/FZKA6984.pdf>
 - 13 Ziegler, J. F.: Particle interactions with matter, <http://www.srim.org/>
 - 14 Pelowitz, D. B.; Durkee, J. W.; Elson, J. S.; Fensin, M. L.; James, M. R.; Johns, R. C.; McKinney, G. W.; Mashnik, S. G.; Waters, L. S.; Wilcox, T. A.; Hendricks, J. S.; Verbeke, J. M.: Report LA-UR-11-02295, April 2011

The authors of this contribution

Alexander Yu. Konobeyev*, Ulrich Fischer, Pavel E. Pereslavytsev
Institute for Neutron Physics and Reactor Technology
Karlsruhe Institute of Technology (KIT)
Hermann-von-Helmholtz-Platz 1
76344 Eggenstein-Leopoldshafen
Germany

* Corresponding author. E-mail: alexander.konobeev@kit.edu

Bibliography

DOI 10.3139/124.110483

KERNTECHNIK

80 (2015) 1; page 7–12

© Carl Hanser Verlag GmbH & Co. KG

ISSN 0932-3902

Books · Bücher

The Radiological Accident in Lia, Georgia. Published by the International Atomic Energy Agency, 2014, ISBN 978-92-0-103614-8, 149 pp., 42.00 EUR.

On 2 December 2001, an accidental overexposure to radiation of three people occurred in a forest approximately 50 km east of Lia, a village in Georgia. The event resulted from the inadvertent use of two hot objects found as personal heaters, which were later found to be two ⁹⁰Sr radioisotope sources with an activity of 1295 TBq. Some 3–3.5 h after their first contact with the sources, the three individuals complained of nausea, headaches, dizziness and vomiting.

One to two weeks later, two of the individuals developed a burning sensation on their backs and one developed the same sensation on his right hand. Their families reported the symptoms to the local police, who advised that they proceed to the local hospital and request medical help. The three individuals were hospitalized on that same day, 22 December 2001, in the city of Zugdidi (the administrative centre of the region). Based on the anamnesis and clinical picture of the three patients, acute radiation syndrome (ARS) was diagnosed, and the case was reported to the Emergency Medical Center in T'bilisi, the capital of Georgia. A request to transfer the patients to the Institute of Hematology and Transfusiology (IHT) in T'bilisi was issued. At the IHT, general treatment was provided to all three patients, which included, among other things, medication for antibacteriological therapy and immunostimulators.

On 4 January 2002, the Government of Georgia requested IAEA assistance under the Convention on Assistance in the Case of a Nuclear Accident or Radiological Emergency (Assistance Convention). Following this request, the IAEA assembled and dispatched two field teams. The first was on 5 January 2002 to discover what had happened (fact finding) and to undertake a preliminary medical evaluation for the prognosis

and treatment of the overexposed individuals. The second was on 27 January 2002 to assist in the training of the recovery team, searching and locating the radioactive sources, implementing the recovery operation, characterizing the radioactive sources, conducting a radiological survey of the accident site and facilitating medical assistance to the overexposed people.

With the help of the IAEA, two of the three patients were later transferred to specialized hospitals abroad. One patient was treated at the Burn Treatment Centre of the Percy Military Training Hospital, in Paris, France, and the other was treated at the Institute of Biophysics of the Burnasyan Federal Medical Biophysical Center, in Moscow, the Russian Federation.

The objectives of this publication are to compile information on the causes and consequences of the accident, make recommendations and disseminate the information – particularly the lessons learned from the event – in order to avoid similar occurrences and to minimize the consequences.

This publication describes the circumstances and events surrounding the accident, its management and the medical treatment of the people exposed. It also describes the dose reconstruction calculations and biodosimetry assessments conducted. A number of uncertainties remain relating to some details of the accident. However, sufficient information.

Background information on the location of the accident, details of the radioactive sources and a chronology of the events are provided in Section 2. The IAEA assistance missions are presented in Section 3, and the recovery of the radioactive sources is discussed in Section 4. Section 5 addresses the results of the biological dosimetry. The medical management of the individuals exposed as a result of the accident, including dose assessment and detailed biodosimetry data, is discussed in Sections 6–9. Section 10 provides a summary of the conclusions and presents recommendations and lessons learned.